Nature Environment and Pollution Technology
An International Quarterly Scientific Journal

p-ISSN: 0972-6268
(Print copies up to 2016)
e-ISSN: 2395-3454

Vol. 21 | No. 1 | pp. 315-319 | 2022

Original Research Paper

https://doi.org/10.46488/NEPT.2022.v21i01.038

Open Access Journal

Exploring the Spatial Pattern of Damage Caused by Typhoon Meranti on the Urban Green Space on Xiamen Island

Huifen Luo*(**)† and Junlin Wu***

*College of Geographical Sciences, Shanxi Normal University, Taiyuan 030000, China

**Department of Geography, Modern College of Humanities and Science of Shanxi Normal University, Linfen 041000, China

***Shanxi Huaye Survey Engineering Technology Co. Ltd., No. 3 Bureau, China Metallurgical Geology Bureau, Taiyuan 030002, China

†Corresponding author: Huifen Luo; luohuif@foxmail.com

Nat. Env. & Poll. Tech.
Website: www.neptjournal.com

Received: 18-12-2021
Revised: 25-02-2021
Accepted: 04-03-2021

Key Words:
Spatial pattern
NDVI
Getis-Ord Gi*
Typhoon Meranti
Xiamen island

ABSTRACT

Typhoons are the main cause of disturbances in the natural environment of coastal cities. Typhoons often damage the urban green space (UGS) of coastal cities, and the spatial pattern of such damages provides important information for disaster recovery. For acquiring such information, remote sensing technology offers a fast and effective means. This study investigated the spatial pattern of typhoon damage to UGS using Sentinel-2 data. To this end, the damage caused by Typhoon Meranti to the UGS of Xiamen Island (including Gulangyu Island) in 2016 was taken as a case study. The results showed that the overall area without vegetation coverage increased by 1159.7 ha. Areas with high vegetation coverage experienced less damage than areas with low vegetation coverage. A coldspot map of damage clusters was generated, and the map showed that severely damaged green areas were distributed in a striped pattern, indicating serious damage to road greening. In terms of direction, east-west roads experienced a higher degree of damage than north-south roads. The determined spatial pattern of the damage caused by Typhoon Meranti on the UGS of Xiamen Island provides a basis for the post-disaster restoration of the landscape of Xiamen Island.

INTRODUCTION

Typhoon disasters are natural disasters caused by tropical cyclones (Lee et al. 2008, Rossi et al. 2013). Particularly in coastal cities, typhoons are the main cause of disturbances to the natural environment. Accordingly, the monitoring of typhoon damage to the natural environment has received extensive attention from scholars. In this regard, research has been conducted considering various aspects, such as the carbon cycle, forest management, and post-disaster recovery process (Lee et al. 2008, Wang et al. 2010, Zhang et al. 2013).

On making landfall, typhoons often damage the urban green space (UGS) of coastal cities. Therefore, the rapid detection of changes in UGS is of great significance for post-disaster reconstruction and garden planning. Compared with field surveys, remote sensing technology is more effective for evaluating the extent and distribution of damage after natural disasters, because it can provide the overall situation of the damage before and after the disaster. Optical remote sensing data is used in the analysis of environmental damage caused by typhoons, focusing on changes in vegetation and land use (Wang et al. 2010, Zhang et al. 2013). The degree of damage to vegetation can be quantitatively evaluated using remote sensing and geospatial analysis methods.

Coastal areas in China are affected by tropical cyclones from the western Pacific and the South China Sea. In 2016, Typhoon Meranti attacked Xiamen Island. In this study, the damage caused by Typhoon Meranti to the UGS of Xiamen was quantitatively analyzed using remote sensing and geospatial analysis methods, and the spatial pattern of the damage was characterized using remote sensing image data. The findings provide deeper insight into the mechanism of typhoon damage, which would serve as a basis for the restoration of the UGS after the disaster.

MATERIALS AND METHODS

Study area and Typhoon Meranti

Xiamen is located in the eastern part of Fujian province, China, on the southeastern edge of the East Asian continent, facing the western Pacific and the South China Sea to the west. Due to its special geographical location and climatic conditions, Xiamen is often hit and affected by typhoons.

The wind is usually strong when typhoons make landfall or impact, which often triggers heavy rainfall, posing serious threats to life and property as well as to economic and social development. In this research, the entire Xiamen Island (including Gulangyu) was taken as the study area. Fig. 1 shows the location of the study area. The Typhoon of Meranti track information is from the Water Resources Department of Zhejiang Province (http://typhoon.zjwater.gov.cn/). The main road is downloaded from Geofabrik GmbH (https://download.geofabrik.de/).

Typhoon Meranti was one of the strongest storms in the global seas in 2016, and it was also the strongest typhoon that landed in southern Fujian since 1949. It landed on the coast of Xiang'an district at 3:05 am on September 15, 2016, with a maximum wind force of 15 (52 $m.s^{-1}$) near the center (http://typhoon.zjwater.gov.cn/). Typhoon Meranti uprooted a large number of trees in Xiamen and damaged green areas, houses, and crops, resulting in a direct economic loss of 10.2 billion Yuan, 28 deaths, 49 injured people, and 18 missing people (Wang & Xu 2018, Wu et al. 2020).

Materials

The 1C level data of two scenes before and after the typhoon were obtained by using Sentinel-2 in the Copernicus Plan of the European Space Agency (ESA) on November 26, 2015, and October 31, 2016 (https://scihub.copernicus.eu/dhus/#/home). In this study, the whole Xiamen Island (including Gulangyu) without cloud cover was taken as the target.

Methodology

Atmospheric correction: Before change detection, Sentinel-2A 1C level data were converted to Sentinel-2A 2A level data, i.e., converting Top of Atmosphere (TOA) reflectance data to Bottom of Atmosphere (BOA) reflectance images. In the experiment, the Sen2Cor (V. 2. 8.0.) module provided by ESA was used to realize atmospheric correction (Main-Knorn et al. 2017). The core algorithm of this module was libRadtran, which is used for calculating radiative transfer in Earth's atmosphere (Mayer & Kylling 2005).

Normalized difference vegetation index: Vegetation indices are used to describe the large-scale distribution and changes in vegetation over a specific area. The normalized difference vegetation index (NDVI) is a commonly used vegetation index, obtained from remote sensing measurements of electromagnetic energy in the red and infrared spectral regions (Ashcroftj et al. 1990, Defries & Townshend 1994). NDVI uses the difference in leaf absorption in the red and near-infrared (NIR) bands. Such measurements are feasible because green vegetation absorbs and reflects more visible red and infrared wavelength radiation. Most spectral vegetation indices are based on some combination of the ratio between the red bands, where chlorophyll absorbs a large amount of incident light and NIR wavelengths, and the latter corresponds to the area of maximum reflectivity of incident radiation, such as healthy green leaves (attributable to their internal mesophyll structure). The advantage of NDVI is that it is seldom affected by the angle of the sun and sunlight, and hence it provides relatively reliable information on the dynamics of vegetation cover. Considering these advantages, we used NDVI to identify and investigate the spatial distribution of green cover in this study. NDVI is the normalized ratio of the NIR and Red bands,

$$NDVI = (\rho_{NIR} - \rho_{Red}) / (\rho_{NIR} + \rho_{Red}) \quad \ldots(1)$$

where the NIR and Red bands correspond to the surface reflectance values of Band8 and Band4 of Sentinel-2A data. The NDVI calculated using this formula ranges from -1.0

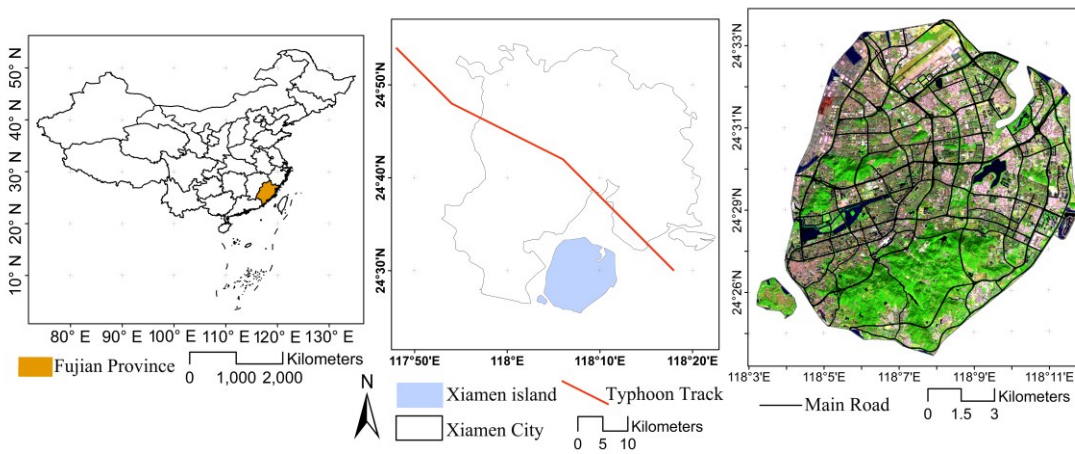

Fig. 1: Location map of the study area and typhoon path map.

to +1.0, with high positive values indicating dense and/or healthy vegetation.

Getis-Ord Gi* of differenced normalized difference vegetation index: Differenced vegetation indices are the most commonly used indices for vegetation change detection. Differenced indices can be used to analyze surface change characteristics before and after typhoons in a quick, simple and quantitative manner. To quantitatively analyze the damage caused by Typhoon Meranti to the UGS of Xiamen Island, the difference between the NDVI of the study area before and after the typhoon was calculated to obtain the dNDVI, i.e., the NDVI value of the post-typhoon image minus that of the pre-typhoon image.

Hotspot analysis was used to calculate Getis-Ord Gi* statistics on the elements of the data, to determine locations of high or low clustering in space (Barrell & Grant 2013, Getis & Ord 1992, Patel et al. 1995, Peeters et al. 2015). As a spatial event, the impact of typhoons on UGS has spatial autocorrelation. With the hotspot analysis, dNDVI was used to determine areas with concentrated vegetation cover, which can reflect the spatial pattern of damage to UGS. The Getis-Ord Gi* formula for calculation is as follows:

$$G_i^* = \left(\sum_{j=1}^{n} w_{i,j}\, x_j - \bar{X} \sum_{j=1}^{n} w_{i,j}\right) \Big/ \left(S * \sqrt{\left[n \sum_{j=1}^{n} w_{i,j}^2 - \left(\sum_{j=1}^{n} w_{i,j}\right)^2\right] / (n-1)}\right) \quad \ldots(2)$$

$$\bar{X} = \sum_{j=1}^{n} x_j / n \quad \ldots(3)$$

$$S = \sqrt{\sum_{j=1}^{n} x_j^2 / n - (\bar{X})^2} \quad \ldots(4)$$

Where x_j is the value of dNDVI, W_{ij} is the Spatial Weigh between i and j, n is the count of the whole image. Statistically significant samples were determined by calculating the Z score based on Getis-Ord Gi* statistics (https://www.esri.com/en-us/arcgis/products/arcgis-pro/resources).

RESULTS AND DISCUSSION

Statistical Analysis of NDVI

Fig. 2 (a) and (b) show spatial distribution maps of the NDVI of Xiamen Island before and after the typhoon. Fig. 2(c) shows the change ratio of vegetation at each level of NDVI before and after the typhoon. The post-typhoon image was taken half a month after the typhoon landed, and grass or crops might have been artificially restored during this period. The average NDVI of all pixels (except the water) of Xiamen Island before the typhoon was 0.3088, and that after the typhoon was 0.2814, reflecting a decrease by 0.0276. The most obvious feature of abrupt canopy detected through optical remote sensing was the loss of leaves, which was directly related to the decrease of NDVI. Although the overall change of NDVI was not large, NDVI tended to be saturated under a high leaf area index, and hence relatively small changes may reflect larger changes on the ground from satellite remote sensing images (Carlson & Ripley 1997).

The area without any vegetation cover (NDVI <0.05) increased by 1159.7 ha according to statistics. Compared with the area before the typhoon, the area without any vegetation cover increased by 17.55-25.67% with a range of 46.28%, accounting for 8.12% of the entire study area. In terms of decreased NDVI, areas with low vegetation coverage showed the largest decrease with a value of 507.6

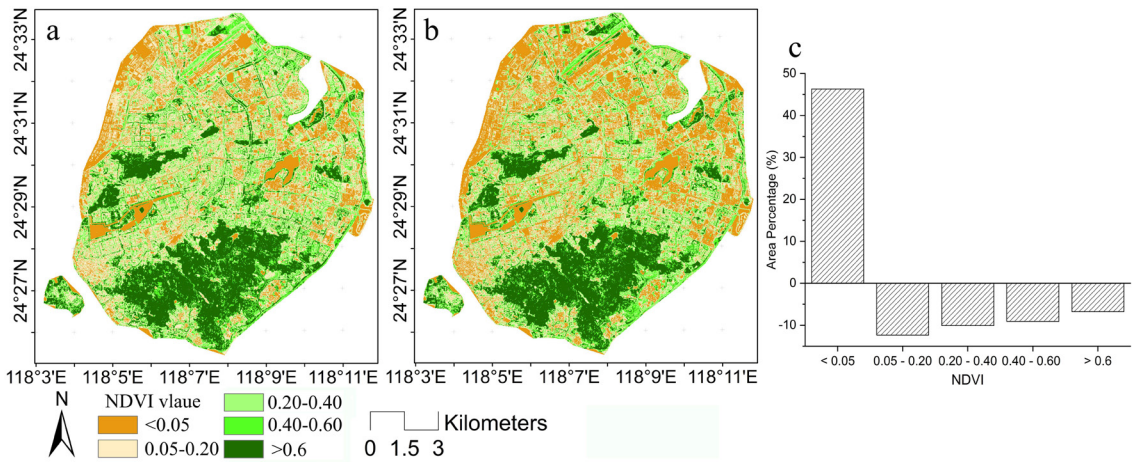

Fig. 2: NDVI (a) before and (b) after Typhoon Meranti; (c) change ratio of vegetation.

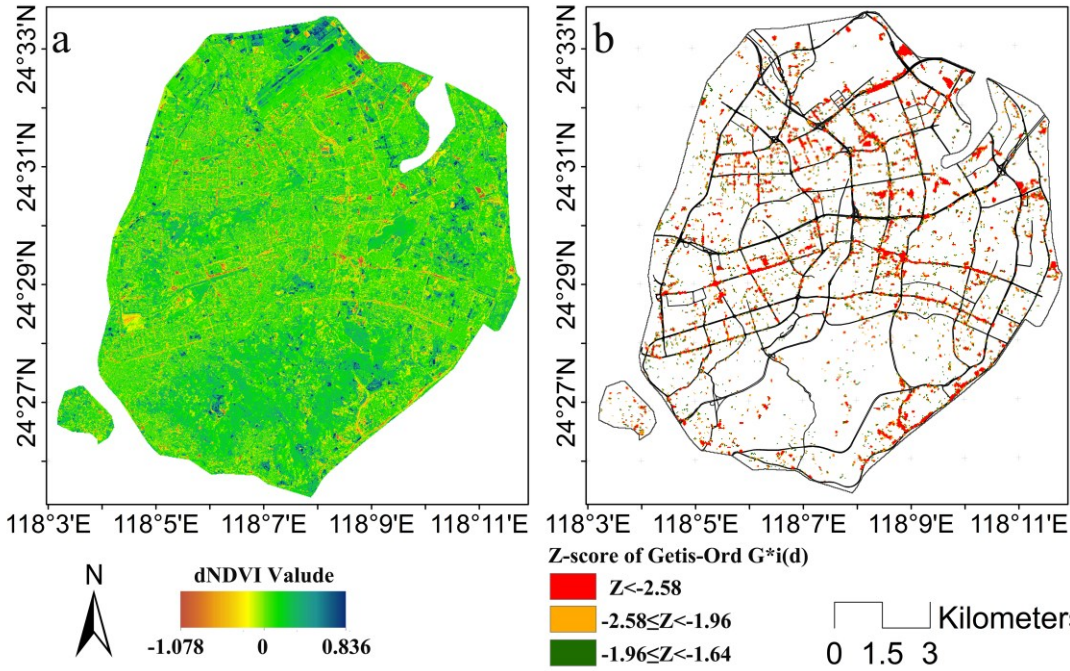

Fig. 3: (a) dNDVI (NDVI-pre subtracting NDVI-post); (b) the coldspots of reduced dNDVI.

ha. Areas with medium, high, and extremely high vegetation coverage decreased by 272.8 ha, 173.3 ha, and 206.0 ha, respectively. From the change ratio of the areas, the rate of change gradually decreased from low vegetation coverage to extremely high vegetation coverage, indicating that areas with low vegetation coverage were seriously affected by typhoons. Areas with high and extremely high vegetation coverage in Xiamen Island mainly include Xiamen Botanic Garden, Dongpingshan Park, and Xianyue Park in the south, Huawei Mountain and Bay Park in the west, the Convention and Exhibition Center and Wuyuan Wetland Park in the east, as well as the Gulangyu Island and some other small parks. Areas with low vegetation coverage area and medium vegetation coverage were mainly community green areas, sidewalk green areas, and small park vegetation. The above data showed areas with high vegetation coverage experienced a lower degree of damage than areas with low vegetation coverage. This result is consistent with the analysis results of Wang & Xu (2018).

Spatial Aggregation Analysis of dNDVI

Fig. 3 (a) shows the difference between the NDVI of the study area before and after the typhoon. dNDVI indicates the change rate of the decrease. As observed, NDVI mainly increased in areas near airports, large parks, and some residential communities, reflecting human intervention to increase UGS. Areas with UGS decrease were consistent with the above NDVI analysis, mainly concentrated in streets and residential communities. Fig. 3(b) shows the coldspot map obtained by analyzing dNDVI data using the hotspot analysis function of ArcGIS software, revealing areas where damages to UGS were concentrated. According to the coldspot map, the damage to UGS in Xiamen Island was distributed in a striped pattern. In other words, heavily affected areas were concentrated along streets (street greening). This might be because the same street planting, tree species, as well as planting methods, such as the level of tree pit depth and tree crown trimming, were usually adopted in urban road vegetation.

Streets with significantly damaged UGS were mainly located in the central and northern parts of the island: Lianqian East Road, Luling Road, and Hubin North Road in the middle, and Fangzhong Road and Fangzhong North Road in the north. These roads have a common characteristic in that they all run east-west. Overall, damaged green areas were rarely concentrated along the north-south roads. The UGS of the southeast section of Huandao East Road showed prominent concentrated damage. However, the sidewalk green space on Xianyue Road, which is the main road running parallel to Hubin North Road with a distance of about 800 m, was not significantly damaged. The distance of Xianyue Road to the typhoon path was farther than that of the southeast

section of Huandao East Road, but the southeast section of Huandao East Road did not show concentrated vegetation damage. We also observed prominent concentrated damage to the green space at the crossroads. The degree of typhoon damage to UGS was related to not only the distance of the road from the typhoon path and wind direction, but also the type of trees and the size of the tree canopy, depth of root system, planting space, and plant conditions.

CONCLUSION

This study investigated the spatial pattern of the damage caused by Typhoon Meranti to the UGS of Xiamen Island, mainly using vegetation index and hotspot analysis. The vegetation index showed that the typhoon seriously damaged the vegetation of Xiamen Island and increased the area without vegetation by 1159.7 ha. Using the coldspot map generated through hotspot analysis, the distribution of areas with concentrated UGS damage could be rapidly determined. The precise spatial aggregation of areas in Xiamen Island affected by Typhoon Meranti could be obtained through the hotspot analysis. From the overall perspective of the spatial pattern, areas with severely damaged UGS were distributed in strips, indicating that road greening was seriously damaged. In terms of direction, areas with severely damaged UGS were more concentrated along east-west roads than along north-south roads. The distribution of severe damage to UGS was not centralized in large parks and other places in high vegetation areas. The determined spatial pattern of the damage caused by Typhoon Meraki to the UGS of Xiamen Island provides a spatial planning basis for urban construction and garden planning of coastal cities similar to Xiamen Island.

ACKNOWLEDGMENTS

This research was financially supported by Scientific and Technological Innovation Programs of Higher Education Institutions in Shanxi, China (Grant No. 2020L0751).

REFERENCES

Ashcroftj, P.M., Cattj, J.A., Curran, P.J., Mundenj, J. and Webster, R. 1990. The relation between reflected radiation and yield on the broad back winter wheat experiment. Int. J. Remote Sens., 11(10): 1821-1836.

Barrell, J. and Grant, J. 2013. Detecting hot and cold spots in a seagrass landscape using local indicators of spatial association. Landsc. Ecol., 28(10): 2005-2018.

Carlson, T.N. and Ripley, D.A. 1997. On the relation between NDVI, fractional vegetation cover, and leaf area index. Remote Sens. Environ., 62(3): 241-252.

Defries, R.S. and Townshend, J.R. 1994. NDVI-derived land cover classifications at a global scale. Int. J. Remote Sens., 15(17): 3567-3586.

Getis, A. and Ord, J.K. 1992. The analysis of spatial association by use of distance statistics. Geogr. Anal., 24(3): 189-206.

Lee, M.F., Lin, T.C., Vadeboncoeur, M.A. and Hwong, J.L. 2008. Remote sensing assessment of forest damage in relation to the 1996 strong typhoon Herb at Lienhuachi experimental forest, Taiwan. Forest Ecol. Manag., 255(8-9): 3297-3306.

Main-Knorn, M., Pflug, B., Louis, J., Debaecker, V., Müller-Wilm, U. and Gascon, F. 2017. Sen2Cor for Sentinel-2, 3: 111

Mayer, B. and Kylling, A. 2005. Technical note: The libRadtran software package for radiative transfer calculations - description and examples of use. Atmos. Chem. Phys., 5(7): 1855-1877.

Patel, K.A., Davis, S.D., Johnson, R. and Esther, C.R. 1995. Local spatial autocorrelation statistics: Distributional issues and an application. Geogr. Anal., 27(4): A3288-A3288.

Peeters, A., Zude, M., Käthner, J., Ünlü, M., Kanber, R. and Hetzroni, A. 2015. Getis-Ord's hot- and cold-spot statistics as a basis for multivariate spatial clustering of orchard tree data. Comp. Electr. Agric., 6: 5-15.

Rossi, E., Rogan, J. and Schneider, L. 2013. Mapping forest damage in northern Nicaragua after Hurricane Felix (2007) using MODIS enhanced vegetation index data. GISci. Remote Sens., 50(4): 385-399.

Wang, M. and Xu, H. 2018. Remote sensing-based assessment of vegetation damage by a strong typhoon (Meranti) in Xiamen Island, China. Nat. Haz., 93(3): 1231-1249.

Wang, W., Qu, J.J., Hao, X., Liu, Y. and Stanturf, J.A. 2010. Post-hurricane forest damage assessment using satellite remote sensing. Agric. Forest Meteorol., 150(1): 122-132.

Wu, K.S., He, Y., Chen, Q.J. and Zheng, Y.M. 2020. Analysis of the damage and recovery of typhoon disaster based on UAV orthograph. Microelectron. Reliab., 107(2019): 113337.

Zhang, X., Wang, Y., Jiang, H. and Wang, X. 2013. Remote-sensing assessment of forest damage by Typhoon Saomai and its related factors at the landscape scale. Int. J. Remote Sens., 34(21): 7874-7886.